DIMUON PRODUCTION BY PIONS AND PROTONS IN IRON AND A SEARCH FOR THE PRODUCTION IN HYDROGEN OF NEW PARTICLES WHICH DECAY INTO MUONS*†

Presented by M. L. Mallary for:

G. J. Blanar□, C. F. Boyer, W. L. Faissler, D. A. Garelick‡, M. W. Gettner, M. J. Glaubman, J. R. Johnson, H. Johnstadδ, M. L. Mallary, E. L. Pothier, D. M. Potter, M. T. Ronan, M. F. Tautz, E. von Goeler and Roy Weinstein
Northeastern University at Boston, Boston, MA 02115

ABSTRACT

Dimuon production cross sections have been measured with a 200 GeV π^- beam and a 240 GeV proton (p) beam. The dimuon mass spectra produced by π and p have essentially the same shape. The dimuon transverse momentum behavior is essentially the same for vector mesons produced by π or by p. For $(\rho+\omega)$ or ψ production the x (Feynman) behavior is approximately independent of the mass of the dimuon produced. The dimuon π production cross section is approximately 6 times greater than that of the p for $x > .5$.

Using a missing mass (M_m) technique, the same pion and proton beams were used to search for the production in hydrogen of new particles which decay with muon emission. Model dependent upper limits (50 to 7000 nanobarns) for the production of such objects with $2.5 < M_m < 7.$ GeV are given (for charmed meson pair production M_m is the mass of the $D\bar{D}$ system).

INTRODUCTION

This talk is a report on the results from two experiments for which the data were collected simultaneously in the M2 beam line of the Meson Laboratory at Fermi National Laboratory. Data were taken with a negative pion beam at a momentum of 200 GeV and a proton beam at a momentum of 240 GeV on the following reactions:

$$\pi^- + Fe \rightarrow \mu^+ + \mu^- + \text{anything} \quad (1)$$

$$p + Fe \rightarrow \mu^+ + \mu^- + \text{anything} \quad (2)$$

$$\pi^- + p \rightarrow p_{recoil} + Y \searrow \mu + \text{anything} \quad (3)$$

$$p + p \rightarrow p_{recoil} + Y \searrow \mu + \text{anything} \quad (4)$$

* Work supported in part by the National Science Foundation under Grant No. MPS70-02059A5.
† Data taken at the Fermi National Accelerator Laboratory.
□ Address: CERN, Geneva, Switzerland.
‡ Supported in part by an Alfred P. Sloan Foundation Fellowship.
δ Address: Faculte des Sciences, Univ. de 1'Etat, Mons, Belgium.

In the data from reactions (1) and (2) the dimuon invariant mass ($M_{\mu\mu}$) spectra were examined for structures from the production of η, ρ, ω, φ, and ψ mesons. For both the $\rho + \omega$ and the ψ, the dependence of the data on longitudinal and transverse momenta were fit to phenomenological forms.

For reactions (3) and (4) the missing mass (M_m) spectra of the system (Y) recoiling against the recoil proton were examined for threshold enhancements in the mass range $2.5 < M_m < 7.$ GeV. Such an enhancement would be evidence for the production of new particles which decay into muons such as charmed particle pairs, vector bosons or heavy lepton pairs. Examples of low mass threshold enhancements have been seen previously for familiar reactions.[1]

Apparatus

The apparatus for these two experiments is shown in Figure 1. It consists of a hydrogen target, a recoil proton spectrometer, and a forward muon spectrometer. Beam optics and counters are not shown. The proton spectrometer[2] measured the recoil proton angles with four magnetostrictive wire spark chambers (SC1 - 4). The proton energy was measured by pulse height analysis of the E counters, in which the protons stopped. The pulse heights from the dE counters were used to identify the stopping particles as protons. The A counters vetoed events in which the protons did not stop. The t acceptance of this spectrometer was $.1 < -t < .4$ GeV^2. The axis of the spectrometer was set at 70^o to the beam giving good acceptance in the missing mass interval $0 < M_m < 7$ GeV. The M_m^2 resolution was 2 GeV^2 FWHM.

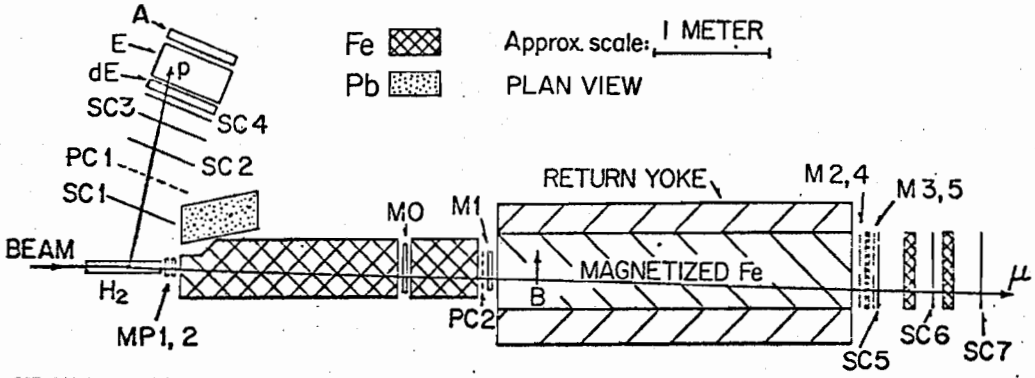

Fig. 1 Plan view of the apparatus. There are five dE, E, and A counters stacked vertically.

The forward muon spectrometer[3] consisted of a 2 m long iron hadron absorber followed by a 56 kilogauss-m magnetized iron spectrometer which bent the muons vertically. Track coordinates were measured in front of the magnet by a multiwire proportional chamber (PC2) and at the rear of the magnet by three magnetostrictive wire spark chambers (SC5 - 7). The trigger for the muon spectrometer required pulses in counters M0·M1·(M2·M3 or M4·M5) for reactions (3) and (4) (at least one muon). For reactions (1) and (2), 1½ minimum ionizing pulse heights were required in M0 and M1 and all of the counters M2·M3·M4·M5 were required (at least two muons). The pulse

heights in counters MP1 and MP2 were used off line to determine the forward charge multiplicity of events from reactions (3) and (4).

In the analysis of the data the muon trajectories were tracked back from the spark chambers to the production point. The momentum was determined from the bend in the vertical plane. In the horizontal plane the tracks were required to extrapolate to within 2.2 s.d. of the production point (errors based on multiple scattering at the measured momentum). In the analysis of the data from reactions (1) and (2) the production point was assumed to be on the beam line at a depth of one absorption length (17 cm) into the iron hadron absorber. For reactions (3) and (4) the production point was assumed to be the beam particle-recoil proton vertex inside the hydrogen target. The muon longitudinal momentum ($P_{\mu\ell}$) was reconstructed to an rms accuracy of approximately $\pm$ 16% and the transverse momenta ($P_{\mu\perp}$) to 0.2 GeV (for $P_{\mu\perp} \lesssim 1$ GeV). The apparatus accepted muons with $P_{\mu\ell} \gtrsim$ 20 GeV and $P_{\mu\perp}/P_{\mu\ell} \lesssim .05$.

Excellent agreement between $P_{\mu\ell}$ and $P_{\mu\perp}$ distribution for data taken on beam muons and the corresponding Monte Carlo distributions gives us confidence in our understanding of the apparatus and the Monte Carlo program.

Dimuon Analysis

In the following analysis the laboratory dimuon longitudinal momentum (P_ℓ) was required to be greater than 90 GeV. This reduces to a negligible level the production of dimuons from the interaction of secondaries in the iron hadron absorber. The dimuon invariant mass spectra from reactions (1) and (2) are shown in Figures 2a and 2b respectively.

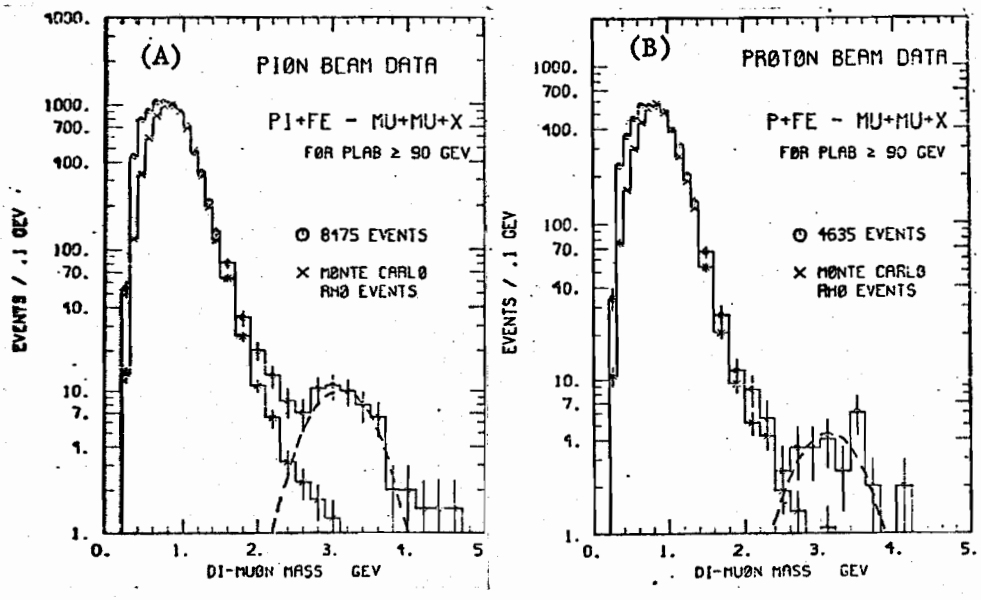

Fig. 2. Di-muon invariant mass spectra a) for reaction (1) and b) for reaction (2).

Also shown along with these spectra are Monte Carlo results (x's) which were generated with a relativistic s-wave Breit Wigner distribution in mass with the parameters of the ρ. The longitudinal and transverse momentum distributions of the Monte Carlo events were chosen to fit the data. The Monte Carlo event sample was normalized to the data in the mass range $1. < M_{\mu\mu} < 1.5$ GeV. From comparisons of the Monte Carlo simulated invariant mass distributions to the data, we conclude that 75% of the total observed dimuon production is consistent with the production of dimuons from the decay of ρ's and ω's (resolution doesn't allow a separation of ρ's from ω's).

In the low mass region ($M_{\mu\mu} \lesssim .6$ GeV) there is a sizable contribution ($\sim 25\%$) consistent with either Bethe Heitler production by γ secondaries or with $\eta \to \mu\mu\gamma$ decays. Monte Carlo studies also indicate that dimuon production from φ's is less than 15% of the ρ + ω dimuon production.[4] In the high mass part of these mass spectra ($2.5 < M_{\mu\mu} < 3.7$ GeV) there are enhancements from ψ(3.1) decay[3]. The dashed curves shown with these spectra are gaussian distributions with widths of 13% rms (which is the ψ resolution expected from Monte Carlo calculations) centered at the ψ mass.

In the analysis of the longitudinal and transverse momentum spectra the events satisfied the longitudinal momentum cut, $P_\ell > 90$ GeV, and mass cuts of $2.5 < M_{\mu\mu} < 3.7$ for the ψ sample and $.77 < M_{\mu\mu} < 1.0$ GeV for the ρ + ω sample. The fits to the spectra were obtained by generating Monte Carlo simulated events with an isotropic center of mass decay distribution. Best fits were then found for phenomenological forms given in Eqs. 5, 6, and 7 below by adjusting the parameters in the Monte Carlo generations until the data was accurately simulated.

The longitudinal momentum distributions were fit to the following forms:

$$\frac{d\sigma}{dx} \alpha\ e^{-ax} \tag{5}$$

and

$$E_{\mu\mu}\ \frac{d\sigma}{dx} \alpha\ (1-|x|)^n \tag{6}$$

where a and n are parameters which were varied; $x = P_{\mu\mu}/P_{max}$; $E_{\mu\mu} = \sqrt{P^2_{\mu\mu} + M^2_{\mu\mu}}$; $P_{\mu\mu}$ is the center of mass longitudinal dimuon momentum and $P_{max} \approx \sqrt{s}/2$. The best fits to these parameters are shown in Table I.[5] The measured cross section per iron nucleus times the muon branching ratio ($\sigma_{90}B$) for $P_\ell > 90$ is also shown in Table I along with the cross section per iron nucleus times the branching ratio ($\sigma_0 B$) for $x > 0$ obtained by extrapolating to $x = 0$ the fits with Equation (6) (preliminary results).

The spectra in dimuon transverse momentum ($P_\perp$) were fit to the form

$$\frac{d\sigma}{dP_\perp^2} \propto e^{-bP_\perp^2} \tag{7}$$

The fits to this form for the $\rho + \omega$ data are shown in Table II.[4]

Table I Fits to the dimuon spectra in x (brackets indicate estimated systematic uncertainties)

Mesons	Beam	a	n	$\sigma_0 B$	$\sigma_{90} B$
				microbarns/Fe nucleus	
$\rho + \omega$	π	$3.5 \pm .2(.5)$	$0.8 \pm .3(.5)$	$51 \pm (26)$	$6.1 \pm (3.)$
$\rho + \omega$	p	$8.8 \pm .3(.5)$	$3.1 \pm .1(.5)$	$45 \pm (23)$	$2.5 \pm (1.3)$
ψ	π	$5.7 \pm .8$	$1.2 \pm .2(.5)$*	$.6 \pm (.3)$*	$.11 \pm (.06)$
ψ	p	9.0 ± 1.5	$4.5 \pm .5$ *	$.7 \pm (.4)$*	$.04 \pm (.02)$

* Preliminary results from a larger data sample than shown in Figs. 2a and b.

Table II Fits to the dimuon spectra in $P_\perp^2$ (brackets indicate systematic uncertainties)

Meson	b(π Beam)	b(p Beam)	$P_\perp^2$ range (GeV^2)
$\rho + \omega$	$2.6 \pm .1(.2)$	$2.1 \pm .1(.2)$	0. - 2.
ψ	$0.8 \pm .2$	$1.1 \pm .3$	0. - 3.

From the fits to the dimuon spectra from Reactions (1) and (2) we find that the $P_\perp$ spectra depend strongly on the meson produced ($\rho + \omega$ or ψ) and weakly on the beam particle whereas the P_ℓ spectra depend strongly on the beam particle and weakly on the meson produced. For forward production $x > .5$, we find pions produce dimuons $5.8 \pm .7$ times more abundantly than protons for $\rho + \omega$ production and 7.4 ± 2.0 times more abundantly for ψ production. This reflects the fact that the pion and proton mass spectra have essentially the same shape.

New Particle Search

Reactions (3) and (4) were examined for threshold effects in the missing mass (M_m) spectra in association with muon production. Such an effect would be indicative of the production of new particles which decay into muons. The missing mass squared spectra for the data from Reactions (3) and (4) are shown in Figures 3a and 3b, respectively (corrected for proton acceptance but not for muon

acceptance). For calibration purposes, data were also taken simultaneously without the muon requirement. The missing mass squared spectra of this data is shown in Figures 3c and 3d.

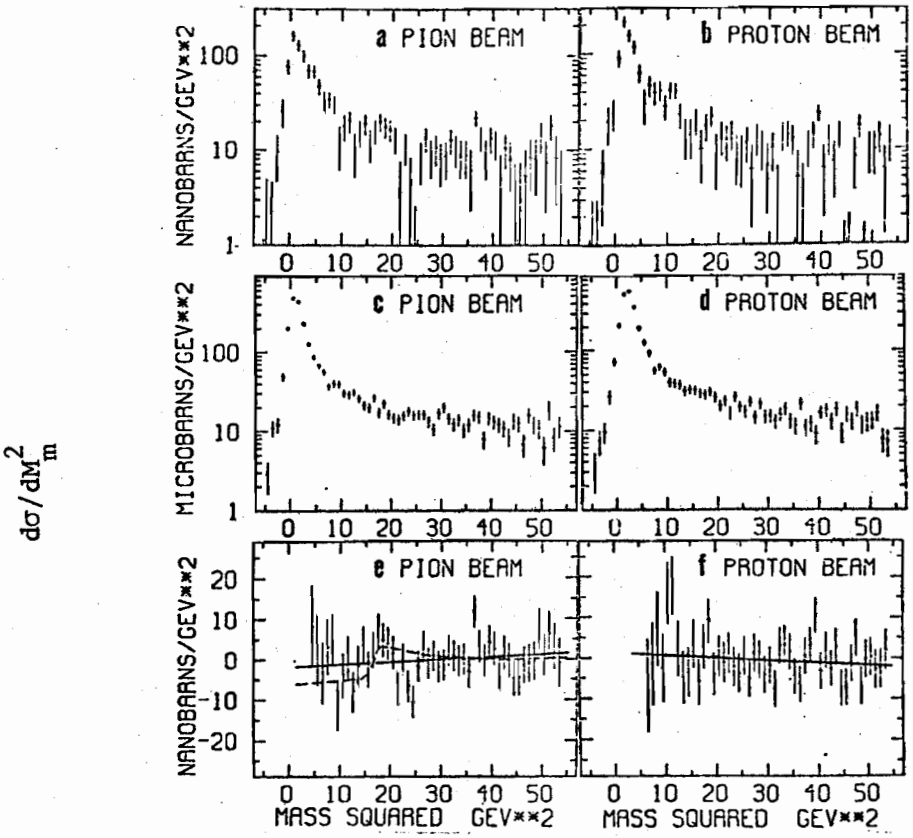

Fig. 3 a) and b) $d\sigma/dM_m^2 = \int (d\sigma/dt dM_m^2) dt$, $.1 < -t < .4$ GeV^2 for Reactions (3) and (4), respectively.

c) and d) $d\sigma/dM_m^2$ for the calibration data (no muon required).

e) and f) $d\sigma/dM_m^2$ difference spectra (see text).

The general features of these spectra are that they are similar in shape but that they differ in magnitude by a factor of about 1000 which is consistent with the expected inflight π and K decay probability. There is an elastic peak, a diffractive peak (not resolved from the elastic peak) which falls as an inverse power of the mass and a flat non-diffractive region.[6] In order to remove the diffractive structure from the spectra in Figure 3a and 3b, for the purpose of bump hunting, the raw mass spectra (not corrected for proton acceptance) of the calibration data (no muon) were fit to the phenomenological form:

$$dN/dM_m^2 = A + BM_m^2 + C/M_m^r \qquad (8)$$

where A, B, C, and r were free fit parameters. The functions which were obtained in this way from the pion and the proton calibration data were then normalized to and subtracted from the corresponding raw mass spectra from Reactions (3) and (4) (in the intervals $4 < M^2 < 54$ GeV^2 for the pion data and $6 < M^2 < 54$ GeV^2 for the proton data). The recoil proton acceptance correction was then made and the resulting difference spectra are shown in Figures 3e and 3f. Straight line fits (solid lines) to these spectra yielded a χ^2 of 49 for 48 d.f. in the pion data and a χ^2 of 45 for 46 d.f. in the proton data. There are no statistically significant structures in these difference spectra.

In order to place upper limits on the production cross section times branching ratio for new particles, the spectra in Figures 3e and 3f were fit to a number of assumed line shapes (smeared with resolution) and 2 standard deviation upper limits were determined. The line shapes used were: a relativistic Briet Wigner to place limits on resonance like production; a step function which rose sharply at threshold and remained constant up to the kinematic limit $M_m^2 \approx 2E_B\sqrt{-t}$ (E_B is the beam energy) to set limits on non-diffractive like production;[6, 7] and a step function which rose sharply at threshold and then fell as a power of the mass ($d\sigma/dM_m^2 \sim 1/M_m^r$) to set limits on diffractive like production.[6, 7] The power, r, was determined from the fits to the calibration data with Equation (8) and was 3.2 for the pion data and 4.0 for the proton data.

The results of this analysis are given in Table III. The entries are the 2 s.d. upper limits on the production cross section (σ_i) times the muon branching ratio (B_μ) times the muon acceptance (A_μ) integrated over the t interval $.1 < -t < .4$ GeV^2 and the mass squared interval $0 < M_m^2 < 2E_B\sqrt{-t}$.

Table III. Upper limits (2 s.d.) on $\sigma_i B_\mu A_\mu$ (in nanobarns).

Beam Particle	Approx. M_m^2(GeV^2)	Resonance Prod. Γ=.05	.2	.8 GeV	Diffractive Production	Non Diffractive Production
π	7	31	43	85	90	3400
π	17	32	62	97	210	1400
π	36	37	54	116	510	1600
π	49	39	58	118	740	1800
p	10	73	92	161	190	3700
p	17	35	44	79	130	1900
p	38	42	57	115	430	2700
p	49	25	44	157	390	1900

To extract upper limits from this table on the total production cross section for massive particles which decay into muons, a specific hypothesis describing the production and decay of these particles is necessary. For example, if charmed meson pairs were produced diffractively[8] by pions, had a branching ratio to muons of unity, decayed to three bodies (e.g. $K\mu\nu$), were produced with a t distribution of $d\sigma/dt \sim e^{-5t}$, and had a mass of 2 GeV (pair mass squared of 16 GeV^2), the relevant entry in the table is 210 nanobarns. This limit is shown as a dashed curve on Fig. 3e. This number is then divided by two to correct for the fact that either meson of the pair can decay, and multiplied by 2 to account for the production outside of the t interval $.1 < -t < .4$ GeV^2. The muon acceptance must also be corrected for, and is then obtained from the following empirical formula:

$$A_\mu = 1 - (M_m/E_B)(5.6\sqrt{E_{cm\mu}} + 9/E_{cm\mu}) \qquad (9)$$

where $E_{cm\mu}$ is the muon center of mass energy in GeV in the forward Y system. For a 2 GeV charm mass and $K\mu\nu$ decay, $E_{cm\mu}$ is about .5 GeV so A_μ is about 0.6. Accounting for these effects, the 2 s.d. limit on diffractive charmed meson pair production, with the above assumptions, deduced from Table III, is 350 nanobarns.

REFERENCES

1. In $\pi + p \rightarrow$ nucleon + x, threshold enhancements are seen when x is: $\pi\rho$ by C. Caso et al., Nuovo Cimento, 54A, 983 (1968); πf by J. Bartach et al., Nuclear Physics, B7, 345 (1968); K^+K^- by B. D. Hyams et al., Nuclear Physics, B22, 189 (1970); and $\bar{p}p$ by G. Grayer et al., Phys. Lett., 39B, 563 (1972).
2. D. Bowen et al., Phys. Rev. Lett. 26, 1663 (1971).
3. G. J. Blanar et al., Phys. Rev. Lett. 35, 346 (1975); Proceedings of the 1975 SLAC Summer Institute on Particle Physics; Proceedings of the Division of Particles and Fields Meeting of the American Physical Society (August 1975) University of Washington, Seattle, Washington; R. Weinstein et al., Proceedings of the 1975 International Symposium on Lepton and Photon Interactions at High Energies, Stanford University.
4. This assumes that $\eta \rightarrow 2\mu$ is small. For an indication of this in pBe see the mass spectra from Yu. M. Antipov et al., Physics Letters, 60B, 309 (1976).
5. These results are described in detail by: M. Ronan, thesis, Northeastern University (1976); and reference (3).
6. F. C. Winkelmann et al., Phys. Rev. Lett. 32, 121 (1974).
7. M. Jacob et al., Phys. Rev. D6, 2444 (1972).
8. The diffractive line shape is a fair approximation to previously observed threshold enhancements (See reference 1).